Effect of Ce doping on structural, magnetic, and transport properties of $SrMnO_3$ perovskite

P. Mandal,[1,2] A. Hassen,[1,3] and A. Loidl[1]
[1]*Experimentalphysik V, Elektronische Korrelationen und Magnetismus, Institut für Physik, Universität Augsburg, D-86159 Augsburg, Germany*
[2]*Saha Institute of Nuclear Physics, 1/AF Bidhannagar, Calcutta 7000064, India*
[3]*Department of Physics, Faculty of Science, Cairo University, Fayoum Branch, Egypt*
(Received 15 September 2003; revised manuscript received 15 March 2004; published 30 June 2004)

We have systematically investigated the structural, magnetic, and transport properties of the $Sr_{1-x}Ce_xMnO_3$ ($0 \leqslant x \leqslant 0.35$) system as a function of temperature and magnetic field. For $x \geqslant 0.10$, the system does not show any long-range magnetic ordering but spin-glass-like behavior at low temperatures below T_{SG}. The in-phase susceptibility χ below T_{SG} decreases and T_{SG} shifts toward higher temperature with the frequency of an ac magnetic field. In the paramagnetic state, χ exhibits an unusual T dependence due to the formation of a microscopic inhomogeneous magnetic phase. For the $x=0.25$ sample, both ρ and χ show an anomaly at around 110 K due to a charge-ordering transition. Both the $x=0.25$ and 0.35 samples show large negative magnetoresistance over a wide range of T.

DOI: 10.1103/PhysRevB.69.224418 PACS number(s): 75.30.Kz, 71.30.+h, 75.50.Lk

I. INTRODUCTION

Mixed-valent manganites $R_{1-x}A_xMnO_3$ (R=rare-earth ion; A=Ba, Sr, Ca, Pb) show fascinating properties due to the correlation between spin, charge, orbital, and lattice dynamics.[1–8] The two end members $RMnO_3$ and $AMnO_3$ are A- and G-type antiferromagnetic (AFM) insulators, respectively. Up to now, most of the studies have concentrated on the R-rich side and very little work has been reported on the Ca- or Sr-rich side.[9–13] Although the electronic configuration remains the same (t_{2g}^3), the AFM transition temperature T_N in $Sr_{1-x}Ca_xMnO_3$ decreases from 233 to 125 K as x increases from 0 to 1 and at the same time the Mn-O-Mn bond angle θ decreases from 180° to 158.8°.[14] T_N can be described as a function of $\cos^2\theta$ related to the superexchange interaction integral and the A-site ionic size variance. In spite of the above differences in structural and magnetic parameters between $SrMnO_3$ and $CaMnO_3$, one expects that the evolution of several physical properties in these two systems on substitution of Sr and Ca with a rare-earth metal will be similar to that of hole-doped manganites ($R_{1-x}A_xMnO_3$).

Maignan *et al.*[12] reported large negative magnetoresistance (MR) in the electron-doped $Ca_{1-x}Ce_xMnO_3$ system. In this compound, the formal valence of the Ce ion is 4, a small amount Ce doping stabilizes a robust ferromagnetic (FM) component in addition to the existing long-range AFM ordering, and a charge-ordering state appears for $0.075 \leqslant x \leqslant 0.20$.[13] The physical properties of $Ca_{1-x}Ce_xMnO_3$ are similar to that of hole-doped manganites.[12,13] As in the case of $Ca_{1-x}Ce_xMnO_3$, doping $SrMnO_3$ with Ce will create Mn^{3+} and eventually introduce a FM double exchange interaction between Mn^{4+} and Mn^{3+} ions and show large negative MR similar to hole-doped manganites. However, Sundarsen *et al.*[15] have shown that the electron-doped $Sr_{1-x}Ce_xMnO_3$ does not show large negative MR and charge ordering. Also the magnetic susceptibility (χ) versus T curve for $x>0.10$ samples shows a broad maximum, which is absent in hole-doped manganites. They have explained this unusual behavior of χ using the dilute AFM model. The differences in magnetic and transport properties between $Sr_{1-x}Ce_xMnO_3$ and hole-doped manganites invoke further studies on this system using single phase samples with classical perovskite structure. With this idea, we have prepared single phase $Sr_{1-x}Ce_xMnO_3$ samples using a two-step method and studied the structural, magnetic, and transport properties over a wide range of temperature and magnetic field. The results are compared and contrasted with earlier reports on $Sr_{1-x}Ce_xMnO_3$ (Refs. 15 and 16) as well as with $Ca_{1-x}Ce_xMnO_3$ (Ref. 13) and hole-doped manganites.

II. SAMPLE PREPARATION AND EXPERIMENTAL DETAILS

Polycrystalline samples of nominal compositions $Sr_{1-x}Ce_xMnO_3$ ($x=0-0.45$) were prepared by using a two-step method reported previously by different groups for the preparation of a similar type of compounds.[10,14] First, stoichiometric proportions of high-purity $SrCO_3$, CeO_2 and Mn_2O_3 were mixed and calcinated at 900 °C to decompose the carbonate, and pressed into pellets at high pressure. The pellets were then heated again at temperatures between 1350 and 1400 °C in flowing argon to obtain oxygen-deficient single-phase samples. This procedure was repeated several times with intermediate grinding. In the second step, these oxygen-deficient samples were annealed at 500 °C in flowing oxygen for a few days, and then slowly cooled to room temperature to obtain oxygen-filled samples. Instead of the two-step method, if we prepare $SrMnO_3$ in air by the conventional one-step solid-state reaction as reported earlier, then the structure becomes hexagonal.[10] The samples were characterized by an x-ray-diffraction (XRD) technique with Cu K_α radiation ($\lambda=1.5406$ Å). Magnetic properties, both dc and ac magnetization, were measured using a SQUID magnetometer (QUANTUM DESIGN) up to a field of 5 T for $2<T<650$ K. The high-field magnetization was measured by a dc extraction method within an OXFORD cryomagnet

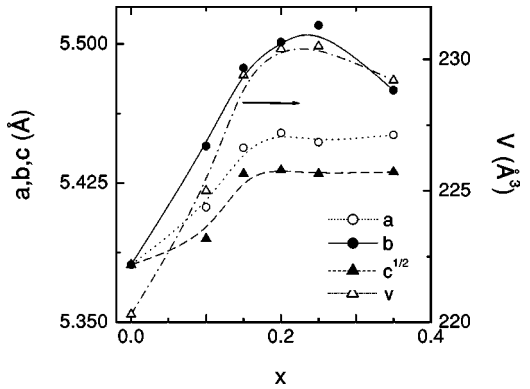

FIG. 1. Variation of lattice parameters a, b, c and the unit-cell volume V with Ce doping (x). The lattice parameters a, b, and c for the $x=0$ sample have been multiplied by $\sqrt{2}$, $\sqrt{2}$, and 2, respectively, to show their systematic evolution with Ce doping.

in fields up to 14 T. The dc electrical resistivity and the magnetoresistance were measured by a standard four-probe technique in the same OXFORD cryomagnet system.

III. EXPERIMENTAL RESULTS AND DISCUSSION

A. Structural analysis

The XRD measurements show that all the samples investigated are of single phase. Above $x=0.35$, a small impurity phase of CeO_2 appears and it increases with increasing x. The XRD pattern of $SrMnO_3$ can be indexed assuming a cubic structure with lattice parameter $a=3.805$ Å, which is close to the reported value.[10,14] A small amount of Ce doping changes the crystal symmetry from cubic to orthorhombic. The volume of the orthorhombic unit cell is four ($\sqrt{2}\times\sqrt{2}\times 2$) times that of the cubic unit cell. In ABO_3, the different lattice distortions can be determined by the tolerance factor $t=(\langle r_A\rangle+\langle r_O\rangle)/[\sqrt{2}(\langle r_B\rangle+\langle r_O\rangle)]$. Here, $\langle r_i\rangle$ represents the ionic size of each element in ABO_3 perovskites. When t is close to 1, the cubic perovskite structure is obtained (e.g., $SrMnO_3$). As Sr^{2+} is partially substituted by Ce^{4+} of smaller size, t decreases from 1 and the lattice symmetry transforms from cubic to orthorhombic, in which the Mn-O-Mn bond angle decreases from 180°.

Figure 1 shows that the lattice parameters do not vary linearly with Ce content x. The parameter b increases with x and shows a broad maximum at around $x=0.25$, close to the critical doping where the charge-ordering state is observed (to be discussed in detail in the subsequent sections). The unit-cell volume V also increases with x and shows a maximum close to $x=0.25$. This anomalous increase of V with the substitution of Ce with smaller ionic radius is due to the creation of Mn^{3+}, which is larger than Mn^{4+}. The dependence of both a and c on x is slightly different from that of b. Initially, a and c increase with the doping and then become almost independent of x above 0.20. Hashimoto and Iwahara[16] observed tetragonal structure up to $x=0.50$, whereas Sundaresan *et al.*[15] reported tetragonal symmetry only for $x\leqslant 0.30$ but orthorhombic beyond 0.30. We believe that these differences in structural properties between the present and earlier works are due to the use of different roots for the sample preparation. In the present work, all the samples were prepared by the two-step method. Samples prepared in this way are of single phase with classical perovskite structure for $0\leqslant x\leqslant 0.35$. On the other hand, samples prepared by the conventional one-step solid state reaction are not single phase for low Ce doping and the structure of $SrMnO_3$ is hexagonal.

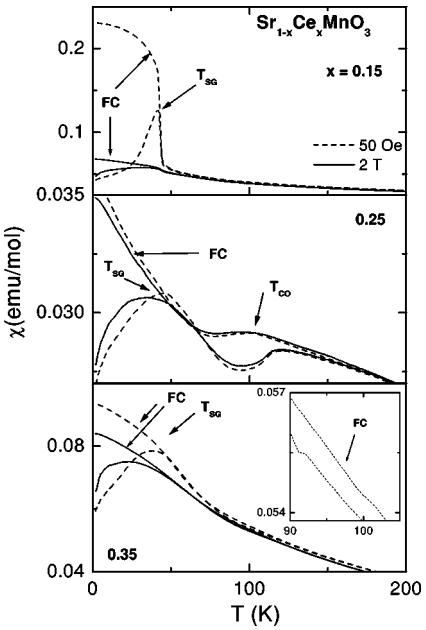

FIG. 2. Temperature dependence of the field-cooled (FC) and zero-field-cooled (ZFC) susceptibility of $Sr_{1-x}Ce_xMnO_3$ for $x=0.15, 0.25$, and 0.35 have been measured at magnetic fields, $H=50$ Oe and 2 T. The spin-glass-like (T_{SG}) and charge-ordering (T_{CO}) transition temperatures are indicated by arrows. Inset shows FC and ZFC susceptibility at 50 Oe close to T_{CO} for $x=0.35$ sample.

B. Magnetic properties

The temperature dependence of zero-field-cooled (ZFC) susceptibility χ_{ZFC} ($=M_{ZFC}/H$) and field-cooled (FC) susceptibility χ_{FC} ($=M_{FC}/H$)) has been measured at different fields for all the samples. In Fig. 2, we present $\chi_{ZFC}(T)$ and $\chi_{FC}(T)$ at two fields $H=50$ Oe and 2 T only for $x=0.15, 0.25$, and 0.35 samples. Neither χ_{ZFC} nor χ_{FC} shows an abrupt increase at low temperature, suggesting the absence of long-range magnetic ordering. On the other hand, the large difference between χ_{ZFC} and χ_{FC}, and the appearance of a cusp in χ_{ZFC} at around $T_{SG}\sim 42$ K, indicates that a spin-glass-like behavior dominates the low-temperature magnetic properties below T_{SG}. It has been observed that when the magnetic field is increased to 5 T, the irreversibility between FC and ZFC susceptibility still exists and the cusp remains. However, the cusp becomes relatively broad and shifts towards the lower temperature. The broadening of the cusp and the decrease of T_{SG} with magnetic field are stronger for $x=0.35$ than 0.25. The $x=0.10$ sample shows a peak in magnetic susceptibility at around 325 K similar to the previous report.[15] This sample

does not show any anomaly at around 295 K due to the AFM ordering[15] but it does show a spin-glass-like transition at around 33 K. T_{SG} becomes zero at 5 T. Also, for $x>0.10$ samples, $\chi(T)$ does not show any broad maximum in the temperature range between 200 and 300 K similar to the previous report.[15] This suggests that in our samples the AFM ordering is suppressed fast with Ce doping and the spin-glass-like state appears around $x=0.10$. The overall T dependence of χ_{ZFC} and χ_{FC} for these samples is similar to other manganites where a spin-glass-like behavior has been reported.[17–22]

In addition to the spin-glass-like behavior at low temperatures, both χ_{ZFC} and χ_{FC} of the $x=0.25$ sample show an additional feature close to 110 K due to the charge-ordering transition. A strong suppression of magnetization from the Curie-Weiss behavior due to the charge-ordering transition below 110 K is clear from Fig. 2. χ_{FC} shows a broad maximum whereas χ_{ZFC} shows a minimum due to the stronger decrease of χ_{ZFC} as compared to χ_{FC}. Similar behavior of magnetization has also been reported for $La_{1-x}Sr_{1+x}MnO_4$ and $Sm_{1-y}Sr_yMnO_3$ systems close to the charge-ordering transition.[19,23] In the vicinity of the charge-ordering transition (T_{CO}), a large irreversibility between FC and ZFC susceptibility is observed even at high fields and χ is slightly enhanced possibly due to the field-induced magnetization. In the $Ca_{1-x}Ce_xMnO_3$ system also, a broad peak has been observed in $\chi(T)$ for $x\geq 0.075$, which has been attributed to the charge-ordering transition.[13] If we assume a Ce^{4+} valence state of Ce in $Sr_{1-x}Ce_xMnO_3$ similar to that in $Ca_{1-x}Ce_xMnO_3$, then $x=0.25$ corresponds to an equal amount of Mn^{3+} and Mn^{4+} ions. This composition is ideal for the occurrence of the charge-ordering phase via the repulsive Coulomb interaction between Mn^{3+} and Mn^{4+}. Normally, the charge-ordering transition is accompanied by the AFM transition, but this has not been observed in the present system. In the $La_{1-x}Sr_{1+x}MnO_4$ system, T_N is suppressed completely above $x=0.2$ as the spin-glass-like phase starts to appear, and for $x\geq 0.5$ the charge-ordering state coexists with the spin-glass-like phase.[19] The qualitative behavior of the T dependence of magnetization for $x\geq 0.5$ samples is similar to the present $x=0.25$ Ce-doped sample.

To understand the low-temperature magnetic behavior more clearly, we have measured the temperature dependence of the ac susceptibility at different frequencies for both 0.25 and 0.35 samples (Fig. 3). Similar to χ_{ZFC}, the real part of ac susceptibility shows a maximum close to T_{SG}. With increasing frequency, the susceptibility decreases and the maximum shifts towards higher temperature. This is a characteristic feature of a spin- or cluster-glass state. We think that a cluster-glass state would be rather more plausible than a spin-glass state, especially in the case of cuprates, manganites, and cobaltates where the tendency of nanoscale electronic phase separation has been clearly demostrated.[24] The glassy state originates possibly due to the competition between the FM double exchange and the AFM superexchange interactions. The average ionic radius $\langle r_A\rangle$ of the A-site ion plays an important role in electronic as well as in magnetic properties because it controls the Mn-O-Mn bond angle, which in turn determines the one-electron bandwidth of the

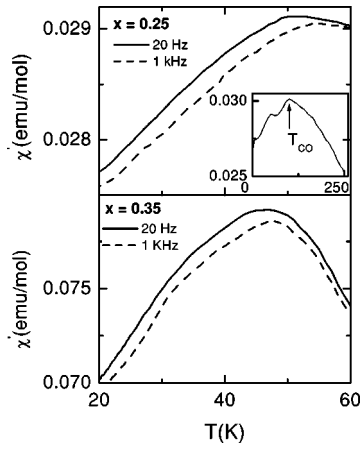

FIG. 3. The real part of ac susceptibility for the $x=0.25$ and $x=0.35$ samples measured at 4 Oe ac magnetic field and at frequencies 20 Hz and 1 kHz as a function of temperature. Inset shows T dependence of χ between 2 and 250 K. The charge-ordering transition is also evident from this curve.

e_g band. With decreasing $\langle r_A\rangle$, the FM transition temperature (T_C) decreases considerably, the system becomes insulating, and shows spin-glass-like behavior below a critical value of $\langle r_A\rangle$.[25] When Sr in $SrMnO_3$ is substituted by Ce with a smaller ionic radius, then $\langle r_A\rangle$ decreases and favors the spin-glass-like state as in the case of other manganites. Ce-doped $CaMnO_3$ does not show any spin-glass-like behavior.[13] This may be due to the smaller ionic radius of Ca as compared to the Sr ion. In this context, it is important to mention that the layered $La_{1-x}Sr_{1+x}MnO_4$ system with K_2NiF_4 structure shows spin-glass-like behavior when La is substituted by a larger-sized Sr ion.[19] This difference between the perovskite and layered manganites may be due to the difference in their crystal structure.

The field dependence of magnetization at different temperatures is shown in Fig. 4. At high temperatures in the PM state $M(H)$ is linear. However, at low temperatures, the field dependence of the isotherms is very different from that of a typical FM system. Below 100 K, $M(H)$ for the $x=0.35$ sample shows a negative curvature. For this sample, the area

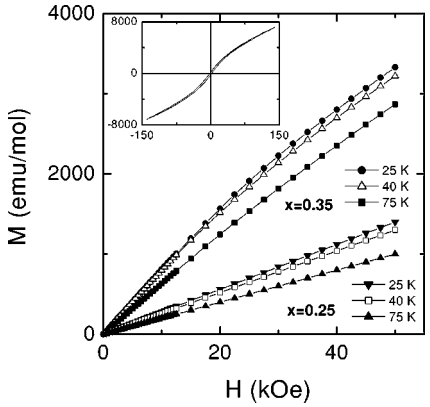

FIG. 4. Magnetic-field dependence of magnetization at different temperatures for $x=0.25$ and 0.35 samples. Inset: hysteresis behavior for the $x=0.35$ sample at 4.2 K up to 14 T.

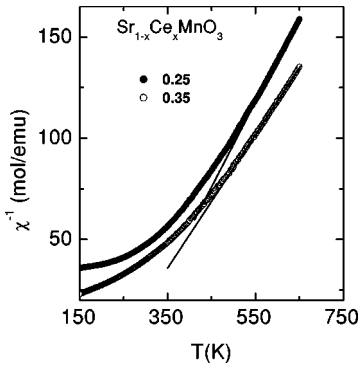

FIG. 5. Temperature variation of inverse magnetic susceptibility (χ^{-1}) for the $x=0.25$ and 0.35 samples in the paramagnetic region. Solid lines show Curie-Weiss behavior for free manganese moments ($C\sim 3$).

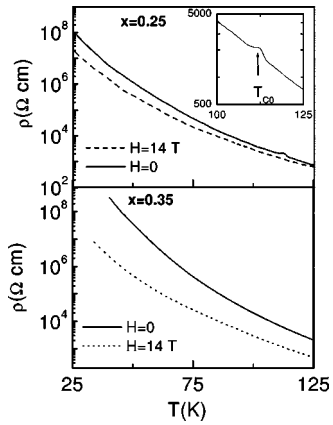

FIG. 6. Resistivity as a function of temperature at different magnetic fields for $x=0.25$ and 0.35 samples. Inset shows a small anomaly in ρ in the vicinity of the charge-ordering transition (T_{CO}) for the $x=0.25$ sample.

of hyteresis loop and the coercive field are very small. Both features are characteristic of the spin-glass-like phase.[26] For the $x=0.25$ sample, $M(H)$ is almost linear over the whole range of field and down to the lowest temperature 4.2 K, and its value at a given field is smaller than that for the 0.35 sample. At low temperatures, the behavior of $M(H)$ of $Sr_{1-x}Ce_xMnO_3$ is very different from that of $Ca_{1-x}Ce_xMnO_3$.[13] In the latter system, a significant amount of spontaneous moment has been observed due to the increase of the FM component with Ce doping, and the spin-only moment of Mn ion is larger than that in $Sr_{1-x}Ce_xMnO_3$. The absolute value of the moment at 4.2 K and at the 14 T field is 1.27 μ_B/Mn for the 0.35 sample. If we assume that the valence state of Ce is 4, then this value is much smaller than the calculated spin-only moment 3.7 μ_B/Mn.

Figure 5 shows $\chi^{-1}(T)$ for the $x=0.25$ and 0.35 samples. In the PM state, the expected Curie-Weiss law for free Mn ions is not observed and $\chi^{-1}(T)$ shows a positive curvature. For both samples, the values of C (Curie constant) determined from the slope of $\chi^{-1}(T)$ at low temperature are much larger than the calculated value using the spin-only moment of the free Mn ion, and θ_p (Weiss constant) is negative. This unusually high value of C implies the formation of magnetic clusters of a few Mn ions together. However, in the material there will be a distribution of cluster size containing Mn^{3+} and Mn^{4+} ions, i.e., an inhomogeneous magnetic phase or nanoscale phase separation. These clusters will grow with decreasing T down to T_{SG}, at which point they freeze due to the severe intercluster frustration and lead to the formation of a spin- or cluster-glass-like state below T_{SG}. The decrease of C with T up to $\sim$500 K is due to the decrease of cluster size. Above 500 K, an approximate linear behavior of $\chi^{-1}(T)$ has been observed with C close to the calculated value ($\sim$3) for free Mn ions. Also, in this temperature range, θ_p becomes positive and the corresponding values of θ_p are 250 and 240 K for the 0.25 and 0.35 samples. For the $x=0.35$ sample, χ shows a small enhancement below 80 K (not shown here). This also indicates a short-range FM interaction between the Mn ions. A positive curvature in $\chi^{-1}(T)$ has been reported for the $Sm_{0.65}Sr_{0.35}MnO_3$ system above T_C.[27] This behavior has been attributed to the formation of small manganese-ion clusters due to the charge and structural fluctuations associated with the inhomogeneous Sr distribution in this compound.

C. Resistivity and magnetoresistance

Figure 6 shows $\rho(T)$ curves for the $x=0.25$ and 0.35 samples at magnetic fields $H=0$ and 14 T. For both samples, ρ increases monotonically with decreasing T down to the lowest temperature measured. $\rho(T)$ for the 0.25 sample shows an anomaly at around 110 K where a broad maximum has been observed in the $M(T)$ curve. Similar behavior has also been observed in the $Ca_{1-x}Ce_xMnO_3$ system close to the charge-ordering temperature.[13] For $x=0.35$, no such anomaly has been observed. This weak anomaly in the vicinity of T_{CO} for the $x=0.25$ sample is suppressed at high magnetic fields. Application of a magnetic field shifts the $\rho(T)$ curves for both samples towards low temperatures, hence producing a large negative MR. The increase of resistivity with Ce doping is possibly due to the decrease of Mn-O-Mn bond angle from 180°.

Fig. 7 shows the temperature dependence of the MR ratio $\Delta\rho/\rho(0)=[\rho(0)-\rho(H)]/\rho(0)$ at 14 T for the $x=0.25$ and 0.35 samples. MR is large over a wide range of T for both samples. Except in the vicinity of T_{CO}, the T dependence of $\Delta\rho/\rho(0)$ for the 0.25 sample is weak. Close to T_{CO}, $\Delta\rho/\rho(0)$ shows a sharp increase due to the suppression of the charge-ordering state with magnetic field. MR for the $x=0.35$ sample decreases monotonically with T. MR of this sample is larger than that for the 0.25 sample. For instance, $\Delta\rho/\rho(0)$ is 99% and 52% at 35 K for the 0.35 and 0.25 samples, respectively. This high value of MR is comparable with that observed in the case of hole-doped manganites and electron-doped $Ca_{1-x}Ce_xMnO_3$.

We have also measured $\rho(H)$ at different T for the 0.25 and 0.35 samples to get a better picture of the nature of the field dependence of MR (Fig. 8). In colossal magnetoresistive materials, $\rho(H)$ shows a positive curvature below T_C.[28,29] The absence of long-range FM ordering is consistent with the absence of the positive curvature in $\rho(H)$ at low tempera-

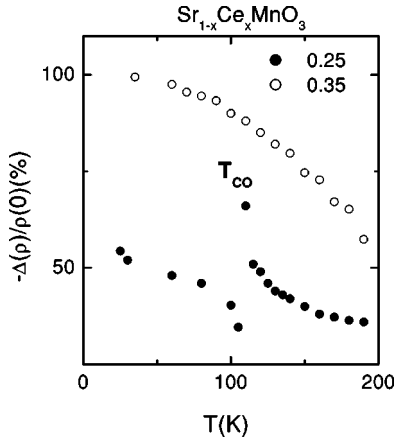

FIG. 7. Temperature dependence of magnetoresistance at 14 T for the $x=0.25$ and 0.35 samples. $\Delta\rho/\rho(0)$ for the $x=0.25$ sample shows a strong anomaly close to the charge-ordering transition T_{CO}.

tures. It is evident from the figure that for the 0.35 sample, a new feature develops in $\Delta\rho/\rho(0)$ versus the H curve above 75 K. Initially, ρ increases with H and then decreases with further increase of H above a field of $\sim 2-3$ T. This effect is absent in the 0.25 sample. Similar to $Sr_{0.65}Ce_{0.35}MnO_3$, $Bi_{1-x}Ca_xMnO_3$ ($x=0.875$) shows positive MR over a narrow range of T at around 100 K.[30] $Bi_{1-x}Ca_xMnO_3$ is a FM insulator and shows charge-ordering. In both systems, positive MR is observed close to a critical doping (x_c) above which the charge-ordering state disappears.[31] Large positive MR has also been observed close to T_{CO} in the case of the FM insulator $La_{0.875}Sr_{0.125}MnO_3$.[4] In this system, positive MR is due to the increase of T_{CO} with H. It has been suggested that T_{CO} increases with H due to the decrease of Jahn-Teller distortion in the FM state. Though $Sr_{0.65}Ce_{0.35}MnO_3$ does not show long-range FM ordering, the positive value of θ_p and the small enhancement of χ below 80 K suggest that the interaction between Mn ions is FM in nature. We believe that the occurrence of positive MR over a narrow range of doping and temperature is due to the subtle interplay between structural, magnetic, and charge-ordering phenomena.

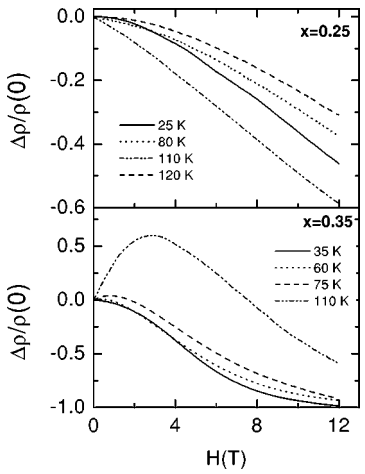

FIG. 8. Magnetic-field dependence of the resistivity at different temperatures for the $x=0.25$ and 0.35 samples.

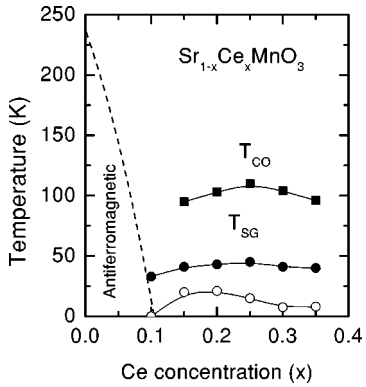

FIG. 9. Magnetic and electronic phase diagram. Transition temperatures, T_{SG} and T_{CO}, determined from magnetic and transport properties are plotted as a function of doping (x). T_{SG} for both $H=0$ (filled circle) and 5 T (open circle) are shown.

It is worthwhile to compare and contrast the evolution of physical properties of Ce-doped $Sr_{1-x}Ce_xMnO_3$ with divalent doped charge-ordering systems. Martin *et al.*[23] have shown that the physical properties of the charge-ordered systems are very sensitive to the A-site mean ionic radius $\langle r_A\rangle$ and the A-site cationic size mismatch, which is quantified by the variance σ^2 of the ionic radii.[32] $\langle r_A\rangle$ of $Sr_{0.75}Ce_{0.25}MnO_3$ is comparable with that for the $Sm_{1-y}Sr_yMnO_3$ and $Pr_{1-y}Sr_yMnO_3$ systems close to $y=0.50$.[23] However, the value of σ^2 is about two and four times larger than the corresponding values for $Sm_{1/2}Sr_{1/2}MnO_3$ and $Pr_{1/2}Sr_{1/2}MnO_3$. Similar to $Sm_{1-y}Sr_yMnO_3$ and $Pr_{1-y}Sr_yMnO_3$, colossal magnetoresistance has been observed in $Sr_{1-x}Ce_xMnO_3$ mainly in the hole-doped region ($x\geqslant 0.25$). The doping range ($0.15\leqslant x\leqslant 0.35$) over which charge-ordering behavior has been observed in $Sr_{1-x}Ce_xMnO_3$ is also comparable with that for $Sm_{1-y}Sr_yMnO_3$. It may be mentioned here that there are also some differences in the physical properties between the two systems. For example, the latter system becomes FM and metallic over a narrow range of doping around $y=0.35$ while the former system does not show any long-range magnetic ordering, and resistivity continues to increase with doping even beyond $x=0.25$. We believe that this behavior of $Sr_{1-x}Ce_xMnO_3$ is due to the decrease of $\langle r_A\rangle$ as well as to the increase of σ^2 with x, which becomes maximum at $x=0.50$. It may be interesting to compare the weak anomaly at around 110 K in the $\rho(T)$ curve of the $Sr_{0.75}Ce_{0.25}MnO_3$ sample with that for $Pr_{0.45}Sr_{0.55}MnO_3$[23], which shows stripelike charge ordering.[33]

D. Phase diagram

Based on the magnetic and transport properties discussed above, a phase diagram has been constructed for $Sr_{1-x}Ce_xMnO_3$, i.e., the dependence of T_{SG} and T_{CO} on doping (Fig. 9). T_{SG} shows a broad maximum at around $x=0.25$ and decreases with the application of a magnetic field. The decrease of T_{SG} is weaker for samples around $x=0.25$ doping. It is also clear from the figure that the spin-glass-like transition can be suppressed completely at magnetic fields higher than 5 T for $x\geqslant 0.30$ as well as for $x<0.15$ samples.

Similar to T_{SG}, T_{CO} also shows a maximum at $x=0.25$. In magnetic measurements, we did not observe an appreciable change in T_{CO} up to the 5 T field.

IV. CONCLUSIONS

The structural, magnetic, and transport properties of the Ce-doped $SrMnO_3$ system have been investigated. Doping with Ce introduces Mn^{3+}, which in turn enhances the double exchange interaction. This affects both magnetic and transport properties dramatically. The magnetic response of $Sr_{1-x}Ce_xMnO_3$ is different from that of ferromagnetic manganite systems, possibly due to the strong competition between the double exchange and superexchange interactions. Both dc and ac magnetization measurements indicate that T_N decreases rapidly with x, and a spin- or cluster-glass-like state appears below T_{SG} for $x \geqslant 0.10$ and T_{SG} decreases with magnetic field. The $x=0.25$ sample shows a charge-ordering transition at around 110 K in magnetization and resistivity measurements. Similar to hole-doped manganites[23] and electron-doped $Ca_{1-x}Ce_xMnO_3$, the $x=0.25$ and 0.35 samples exhibit a large negative magnetoresistance over a wide range of temperature. We have observed some similarities as well as important differences between our and pervious results on structural, transport, and magnetic properties of $Sr_{1-x}Ce_xMnO_3$. In an earlier report, neither the magnetization nor the resistivity measurement shows the charge-ordering phenomenon in this system. This may be due to the use of different methods for the sample preparation.

ACKNOWLEDGMENTS

We thank D. Vieweg, M. Müller, and A. Pimenova for the technical help during the measurements in SQUID and the x-ray diffractometer. This work was supported by the BMBF via Contract No. EKM 13 N 6917 and partly by the Deutsche Forschungsgemeinschaft.

[1] S. Jin, T. H. Tiefel, M. McCormack, R. A. Fastnacht, R. Ramesh, and L. H. Chen, Science **264**, 413 (1994).
[2] P. Schiffer, A. P. Ramirez, W. Bao, and S.-W. Cheong, Phys. Rev. Lett. **75**, 3336 (1995).
[3] A. Urushibara, Y. Moritomo, T. Arima, A. Asamitsu, G. Kido, and Y. Tokura, Phys. Rev. B **51**, 14 103 (1995).
[4] S. Uhlenbruck, R. Teipen, R. Klingeler, B. Büchner, O. Friedt, M. Hücker, H. Kierspel, T. Niemöller, L. Pinsard, A. Revcolevschi, and R. Gross, Phys. Rev. Lett. **82**, 185 (1999).
[5] A. J. Millis, P. B. Littlewood, and B. I. Shraiman, Phys. Rev. Lett. **74**, 5144 (1995).
[6] H. Röder, J. Zang, and A. R. Bishop, Phys. Rev. Lett. **76**, 1356 (1996).
[7] I. Solovyev, N. Hamada, and K. Terakura, Phys. Rev. Lett. **76**, 4825 (1996).
[8] A. J. Millis, Nature (London) **392**, 147 (1998).
[9] B. Fisher, L. Patlagan, G. M. Reisner, and A. Knizhnik, Phys. Rev. B **61**, 470 (2000).
[10] K. Kikuchi, H. Chiba, M. Kikuchi, and Y. Syono, J. Solid State Chem. **146**, 1 (1999).
[11] J. L. Cohn and J. J. Neumeier, Phys. Rev. B **66**, 100404 (2002).
[12] A. Maignan, C. Martin, F. Damay, and B. Raveau, Chem. Mater. **10**, 950 (1998).
[13] Z. Zeng, M. Greenblatt, and M. Croft, Phys. Rev. B **63**, 224410 (2001).
[14] O. Chmaissem, B. Dabrowski, S. Kolesnik, J. Mais, D. E. Brown, R. Kruk, P. Prior, B. Pyles, and J. D. Jorgensen, Phys. Rev. B **64**, 134412 (2001).
[15] A. Sundaresan, J. Tholence, A. Maignan, C. Martin, M. Hervieu, B. Raveau, and E. Suard, Eur. Phys. J. B **14**, 431 (2000).
[16] H. Hashimoto and H. Iwahara, J. Electroceram. **4**, 225 (2000); Mater. Res. Bull. **35**, 2253 (2000).
[17] X. L. Wang, J. Horvat, H. K. Liu, and S. X. Dou, J. Magn. Magn. Mater. **182**, L1 (1998).
[18] R. Mathieu, P. Nordblad, D. N. H. Nam, N. X. Phuc, and N. V. Khiem, Phys. Rev. B **63**, 174405 (2001).
[19] Y. Moritomo, Y. Tomioka, A. Asamitsu, and Y. Tokura, Phys. Rev. B **51**, 3297 (1995).
[20] A. Maignan, U. V. Varadaraju, F. Millange, and B. Raveau, J. Magn. Magn. Mater. **168**, L237 (1997).
[21] J. M. De Teresa, M. R. Ibarra, J. Garcia, J. Blasco, C. Ritter, P. A. Algarabel, C. Marquina, and A. del Moral, Phys. Rev. Lett. **76**, 3392 (1996).
[22] A. Sundaresan, A. Maignan, and B. Raveau, Phys. Rev. B **55**, 5596 (1997).
[23] C. Martin, A. Maignan, M. Hervieu, and B. Raveau, Phys. Rev. B **60**, 12 191 (1999).
[24] A. Moreo, S. Yunoki, and E. Dagotto, Science **283**, 2034 (1999); in the proceedings of the workshop on *Intrinsic Multiscale Structure and Dynamics in Complex Electronic Oxides*, edited by A. R. Bishop, S. R. Shenoy, and S. Sridhar (World Scientific, Singapore, 2002); P. L. Kuhns, M. J. R. Hoch, W. G. Moulton, A. P. Rayes, J. Wu, and C. Leighton, Phys. Rev. Lett. **91**, 127202 (2003).
[25] H. Y. Hwang, S.-W. Cheong, P. G. Radaelli, M. Marezio, and B. Batlogg, Phys. Rev. Lett. **75**, 914 (1995).
[26] G. A. Petrakovskii, K. S. Aleksandrov, L. N. Bezmaternikh, S. S. Aplesnin, B. Roessli, F. Semadeni, A. Amato, C. Baines, J. Bartolome, and M. Evangelisti, Phys. Rev. B **63**, 184425 (2001).
[27] R. P. Borges, F. Ott, R. M. Thomas, V. Skumryev, J. M. D. Coey, J. I. Arnaudas, and L. Ranno, Phys. Rev. B **60**, 12 847 (1999).
[28] Y. X. Jia, L. Lu, K. Khazeni, V. H. Crespi, A. Zettl, and M. L. Cohen, Phys. Rev. B **52**, 9147 (1995).
[29] J. O'Donnell, M. Onellion, M. S. Rzchowski, J. N. Eckstein, and I. Bozovic, Phys. Rev. B **54**, R6841 (1996).
[30] H. Chiba, M. Kikuchi, K. Kusaba, Y. Muraoka, and Y. Syono, Solid State Commun. **99**, 499 (1996).
[31] H. Woo, T. A. Tyson, M. Croft, S.-W. Cheong, and J. C. Woicik, Phys. Rev. B **63**, 134412 (2001).
[32] L. M. Rodriguez-Martinez and J. P. Attfield, Phys. Rev. B **54**, R15622 (1996).
[33] R. Kajimoto, H. Yoshizawa, Y. Tomioka, and Y. Tokura, Phys. Rev. B **66**, 180402 (2002).